Observation of novel patterns in a stressed lattice-gas model of swarming

Olivier Bouré, Nazim A. Fatès, Vincent Chevrier

Observation of novel patterns in a stressed lattice-gas model of swarming

Olivier Bouré – olivier.boure@loria.fr
Nazim Fatès – nazim.fates@loria.fr
Vincent Chevrier – vincent.chevrier@loria.fr

Nancy Université – INRIA Nancy–Grand Est – LORIA

October 23, 2011

Abstract

This paper intends to revisit the behaviour of a lattice-gas cellular automaton model of swarming, in which particles are oriented according to an interaction rule that favours local alignment. This model has been shown to display a phase transition between an ordered and a disordered phase in a parametrical plane of the particle density and alignment sensitivity. We "stress" this model by setting extreme values for these parameters and observe the emergence of novel organised patterns which, surprisingly, do not necessarily maximise the global motion of particles. We show that even with the model being stochastic and simple, the self-organisation process can result in a variety of behaviours. We discuss these observations in the light of the study of discretisation effects.
Note: All quantitative simulations and visualisations were made with the *Fiatlux* CA simulator (`fiatlux.loria.fr`). For visualisations of the system evolution, see additional electronic materials at `www.loria.fr/~boure/swarmlgca/`
Keywords: Swarming behaviour; Lattice-gas cellular automata; phase transitions; robustness; discretisation effects.

Introduction

Swarming behaviour, characterised as the collective motion of aligned entities based on local interaction rules, roots from the work of Renoylds. In 1986 he created *Boids*, a program that simulates a flock of birds based on three base steering behaviours: separation, alignment and cohesion [1]. Since then, this idea of collective motion emerging from a decentralised organisation has been applied for problem solving [2, 3], as well as biological modelling in a wide range of fields stretching from microbiological phenomena [4, 5, 6] to crowd simulation [7, 8]. But if original simulations comprised up to a few dozens

agents, biological systems are made up of thousands of interacting individuals, which calls for large-scale simulations. As the increase of computational power alone was not sufficient to carry them out, the interest quickly turned to lighter, computationally simpler models of swarming. The advantage is two-fold: first, simple models allow us to explore quickly a broader range of rules, and to obtain good statistical data by repeating experiments. Second, reproducing complex phenomena with simple models may help us to identify more precisely the role played by each parameter that defines the model.

Two main methods have been used to simplify models to analyse biological phenomena. A first step lies in the simplification of the individual rule. For the swarming model, in 1995, Vicsek *et al.* introduced a model of "self-propelled particles" moving at constant speed in a continuous space [9]. The authors observed that a local direction averaging rule could exhibit a phase transition from local swarming to a complete alignment of the particles. More recently, Peruani *et al.* proposed an explanation for the phase transition of self-propelled particles using mean-field theory [10]. In this case, simplifying the model made possible to find similarities between the phenomenon and existing tools from statistical physics.

Discretising the space is a second step to simplify further a model. Spatially-discrete systems such as lattice-gas cellular automata (LGCA) are well-suited tools for simulating complex systems because of their parallel, spatially-extended structure. Several lattice-gas versions of Vicsek's self-propelled particles were developed by Deutsch *et al.* [11, 12] as well as Csahók and Vicsek [13]. These models show a conservation of the phase transition for discrete lattices, though the observation of the resulting behaviour is somewhat different from the continuous space version.

The use of a discrete model for space inevitably alters the way entities interact and therefore constitutes a potential source of bias that could affect dramatically the system's behaviour. In such a context, one may thus want to distinguish the behaviour "truly" related to the biological phenomenon from those induced by the simulation conditions of a simplified model [14]. An intuitive method for detecting such effects consists in "stressing" the model, that is, modifying modularily certain aspects of the model and looking for behavioural changes. For instance, the influence of discrete modelling of traffic systems has been studied by D'Souza for the geometry of the lattice [15], and Kirchner *et al.* for the change of granularity [16]. Similarly, Schönfish and Vlad, as well as Grilo and Correia, have shown examples in Biology where the updating scheme plays an essential role in the dynamics of cellular automata models [17, 18].

We thus ask the question of the robustness of the LGCA swarming model, that is, to what extent it is dependent on the attributes of the model.

This paper is divided into five sections. We formally define the model in Sec. 1 and then present the reference results obtained by Bussemaker *et al.* [11] in Sec. 2. Our contribution is introduced in Sec. 3, where we stress the model by choosing specific settings for the alignment sensitivity and the initial particle density. By introducing new behaviour monitoring tools, we show that novel behaviours appear. In Sec. 4, we try to estimate the role of the lattice in the

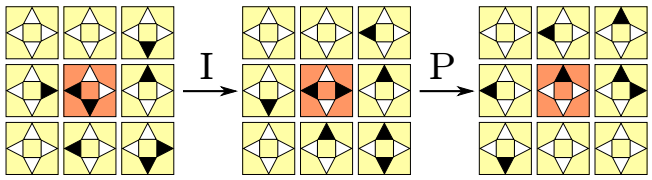

Figure 1: The cycle of a LGCA cell (a) at initial state, (b) after Interaction step, (c) after Propagation step. By convention, black and white triangles represent occupied and empty channels respectively.

formation of these behaviours. Finally, we discuss the system behaviour in the light of our observations in Sec. 5.

1 A lattice-gas model of the Swarm

1.1 Lattice-Gas Cellular Automata

A lattice-gas cellular automaton (LGCA) is a discrete dynamical system defined by a triplet $\{\mathcal{L}, \mathcal{N}, f_I\}$ where :

- $\mathcal{L} \subset \mathbb{Z}^2$ is the array that forms the cellular space.
- $\mathcal{N}$ is a finite set of vectors called the *neighbourhood*. It associates to a cell the set of its neighbouring cells. The sets $\mathcal{N}$ and $\mathcal{L}$ are such that for all $c \in \mathcal{L}$ and for all $n \in \mathcal{N}$, the *neighbour* $c + n$ is in $\mathcal{L}$.
- f_I is the *local interaction rule*.

In lattice-gas cellular automata, neighbouring cells are connected via *channels* through which *particles* can travel from one cell to another. For the sake of simplicity, we will consider here that each channel is associated to a neighbour. Consequently, the number of channels is given by $\nu = \text{card}(\mathcal{N})$.

A *configuration* $\boldsymbol{x}$ denotes the state of the automaton; it is defined as a function $\boldsymbol{x} : \mathcal{L} \to \mathcal{Q} \subset \mathbb{N}^\nu$ which maps each cell to a set of states for the channels. Each channel contains a given number of particles represented by an element of $\mathbb{N}$. The state of a cell $c \in \mathcal{L}$ is denoted by $\boldsymbol{x}_c = (x_1(c), ..., x_\nu(c)) \in \mathcal{Q}$, where $x_i(c) \in \mathbb{N}$ is the state of the i-th channel that connects cell c and its neighbour $c + n_i$, with $\mathcal{N} = \{n_1, \ldots, n_\nu\}$.

The dynamics of a LGCA arises from the successive applications of two transitions applied to all cells synchronously (see example on Fig. 1):

- The *interaction step* I reorganises the particles within each cell.
  The result of the local transition $f_I : \mathcal{Q}^{\nu+1} \to \mathcal{Q}$ is denoted by:

$$\boldsymbol{x}_c^I = f_I(\boldsymbol{x}_c, \boldsymbol{x}_{c+n_1}, \ldots, \boldsymbol{x}_{c+n_\nu}), \text{ with } \mathcal{N} = \{n_1, \ldots, n_\nu\}. \qquad (1)$$

- The *propagation step* P relocates all particles simultaneously in the same channel of the corresponding neighbour in $\mathcal{N}$.
  The result of the local transition $f_P : \mathcal{Q}^{\nu+1} \to \mathcal{Q}$ is given by:

$$\begin{aligned} \boldsymbol{x}_c^P &= f_P(\boldsymbol{x}_c^I, \boldsymbol{x}_{c+n_1}^I, \ldots, \boldsymbol{x}_{c+n_\nu}^I) \\ &= \big(x_1^I(c-n_1), \ldots, x_\nu^I(c-n_\nu)\big) \end{aligned} \tag{2}$$

The evolution of the system from a time t to the following time $t+1$ is determined by: $\boldsymbol{x}^{t+1} = P \circ I(\boldsymbol{x}^t)$. In this paper, initial configurations $\boldsymbol{x}^0$ are generated from a uniform distribution of *density* ρ, where ρ is the probability for *each channel*, independently, to contain a particle.

1.2 Swarm in Lattice-Gas Cellular Automata

The swarm model we study is taken from the work of Deutsch *et al.* compiled in a dedicated book (see [12], chapter 8.2). It describes a probabilistic *swarming interaction* rule in which a cell reorganises its particles according to a probability distribution that maximises local alignment.

This transition is particle-conserving and uses its neighbourhood state as a director field to align the cell particles. In this paper, the neighbourhood is composed of the vectors of the 4 nearest cells: $\mathcal{N} = \{(1,0),(0,1),(-1,0),(0,-1)\}$. Moreover, an *exclusion principle* is imposed: a channel contains at most one particle. As a consequence, a configuration is a vector $\boldsymbol{x} \in \mathcal{Q}^{\mathcal{L}}$ where the state for a cell c is a vector $\boldsymbol{x}_c \in \mathcal{Q} = \{0,1\}^4$.

To maximise the alignment of particles within cells, the computation of the individual rule uses two parameters:

(a) The *local flux* $J_c(\boldsymbol{x})$ denotes the resulting particle direction in a cell c:

$$J_c(\boldsymbol{x}) = \sum_{i=1}^{\nu} x_i(c) \cdot n_i \tag{3}$$

(b) The *director field* $D_c(\boldsymbol{x})$ denotes the total flux of the neighbourhood of a cell c:

$$D_c(\boldsymbol{x}) = \sum_{i=1}^{\nu} J_{c+n_i}(\boldsymbol{x}) \tag{4}$$

The *local alignment* γ is defined as the scalar product of a flux $j \in \mathbb{R}^2$ with a director field $d \in \mathbb{R}^2$:

$$\gamma(j,d) = j \cdot d \tag{5}$$

Let $k(\boldsymbol{x},c) = \sum_{i=1}^{\nu} x_i(c)$ be the the number of particles in a cell, and $\Omega(k) \subset \mathcal{Q}$ the possible states of a cell that contains k particles. For a cell $c \in \mathcal{L}$, the

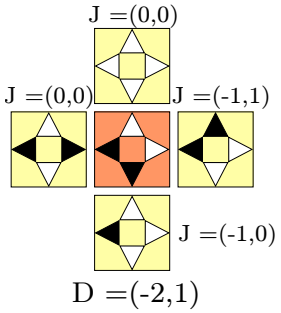

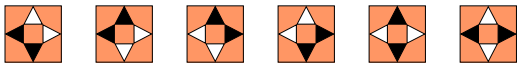

α	e^{α}	$e^{3\alpha}$	$e^{-\alpha}$	$e^{-3\alpha}$	e^{0}	e^{0}
0.5	1.65	4.48	0.06	0.02	1	1
1.5	4.48	90	0.02	0.01	1	1
4	54.6	10^{5}	0.01	10^{-6}	1	1

Figure 2: Example of the application of the swarm interaction rule for the central cell. Left: typical states for a cell and its neighbours, with neighbouring fluxes (Eq. 3) and the director field $D_c(\boldsymbol{x})$ of the center cell (Eq. 4). Right: elements of $\Omega(2)$ and their associated alignment γ (Eq. 5), along with a table of the computed weights (Eq. 6) for different values of α before normalisation to probability.

transition probability for the interaction step to update from a state $\boldsymbol{x}_c$ to a new state $\boldsymbol{x}_c^I \in \Omega(k(x,c))$ in the presence of the director field $D_c(\boldsymbol{x})$ is given by:

$$P(\boldsymbol{x_c} \to \boldsymbol{x}_c^I) = \frac{1}{Z}\exp\Big[\alpha \cdot \gamma\left(J_c(\boldsymbol{x}^I), D_c(\boldsymbol{x})\right)\Big] \tag{6}$$

where:

- The normalisation factor Z is such that $\sum_{\boldsymbol{x}_c^I \in \Omega(k(x,c))} P(\boldsymbol{x}_c \to \boldsymbol{x}_c^I) = 1$.
- The *alignment sensitivity* α is a control parameter that varies the intensity of the swarming effects.

An example of the application of the rule is shown on Fig. 2. Note that when $\alpha = 0$, all outcomes $\boldsymbol{x}^I \in \{0;1\}^{\nu}$ that conserve the number of particles have an equal probability to be selected, regardless of their direction. The evolution of the system will therefore be completely random. Inversely, when $\alpha \to \infty$, the system becomes almost deterministic, that is, the selection always picks one of the configurations that maximises the local alignment.

1.3 Monitoring the behaviour

To quantify the behaviour of our system, two different order parameters have been used:

1. The *mean velocity* $\overline{\phi}$, introduced by Bussemaker *et al.*, averages horizontal and vertical momentum, in order to quantify a consensus in direction of particles. For a configuration $\boldsymbol{x}$, it is defined by:

$$\overline{\phi}(\boldsymbol{x}) = \frac{1}{\mathrm{card}(\mathcal{L})}\left\|\sum_{c\in\mathcal{L}}(J_c(\boldsymbol{x}))\right\|_{\infty} \tag{7}$$

where $\|\boldsymbol{v}\|_\infty = |v_x| + |v_y|$.

2. To this parameter, we added the *mean alignment* $\overline{\gamma}$ to express whether particles are in average aligned with the flux of its neighbour:

$$\overline{\gamma}(\boldsymbol{x}) = \frac{1}{k(\boldsymbol{x})} \sum_{c \in \mathcal{L}} \frac{1}{\mathrm{card}(\mathcal{N})} \gamma(J_c(\boldsymbol{x}), D_c(\boldsymbol{x})) \tag{8}$$

where $k(\boldsymbol{x}) = \sum_{c \in \mathcal{L}} k(\boldsymbol{x}, c)$ is the total number of particles. Its value varies in $[-1, 1]$: $\overline{\gamma} = 1$ indicates that all particles are aligned, and for $\overline{\gamma} = -1$, all particles are antialigned[1].

It should be noted that these two parameters are complementary because they deal with two distinct aspects of the spatial organisation of particles: the mean alignment $\overline{\gamma}$ monitors the average local alignment, whereas the mean velocity $\overline{\phi}$ captures a more global direction consensus. An example of typical values of order parameters for qualitatively different configurations is given on Fig. 3.

In addition, three types of visualisation are used to display the configurations (see for example Fig. 4):

- The *density visualisation* displays how many particles are in a cell. Empty cells are white, cells with 1, 2 and 3 particles are light, medium or dark gray, respectively, and fully occupied cells with 4 particles are black.
- The *flux visualisation* is a new representation that we introduce in order to facilitate the reading of the resulting particles direction within cells by associating a color for each cell flux. A zero-flux cell is represented in white, while other types of flux show a different color for each corresponding cardinal point: N (green), N-E (lime), E (yellow), S-E (orange), S (red), S-W (magenta), W (blue), N-W (cyan).
- The *channel visualisation* displays the state of channels within cells by showing an oriented full triangle when a particle is present in a channel.

2 Known phenomena in the swarm instability

The model of swarming described above displays a qualitative change of behaviour in the continuous domain of the alignment sensitivity α and initial density ρ. This phenomenon was observed by Bussemaker, Deutsch and Geigant [11]. Let us first recall their main results, reproducing the experiments with our own simulation environment.

[1] We borrow this term from spins systems in particle physics. Antialignment refers to the relationship between two particles whose directions are on the same axis, but in opposition.

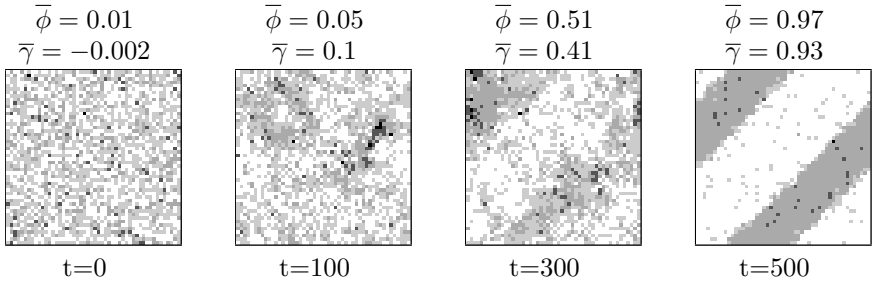

Figure 3: Density visualisation of configurations at different times and corresponding values of the order parameters, for $\alpha = 1.5$, $\rho = 0.2$, $L = 50$. In the ordered phase, the swarm LGCA models starts to form small clouds of particles, which by means of conflicting and synchronising, end up forming a single stripe.

2.1 Description of the emerging pattern

We first take a square-shaped lattice with periodic boundary conditions, that is, we set $\mathcal{L} = (\mathbb{Z}/L\mathbb{Z})^2$, and set the initial particle density to $\rho = 0.2$ and the swarming sensitivity to $\alpha = 1.5$. The evolution of the system configuration for a few hundreds steps displays a emerging phenomenon (see Fig. 3). Starting from a random initial distribution, particles start forming small clusters which travel across the lattice. Due to the periodic boundaries conditions, they cross and interact regularly with a period equal to the lattice size. After several periods, these clusters influence each other until a consensus is found: a stable (but not static) organised pattern appears. It can be described as follows:

Traveling diagonal stripe pattern. This stable behaviour has the shape of a diagonal stripe that loops spatially over the periodic boundaries of the lattice, and is composed of cells containing two particles, which all point to two orthogonal directions. The resulting pattern travels diagonally through the lattice in the combined directions of the particles. It is quantitatively characterised by high values for both mean velocity $\overline{\phi}$ and mean alignment $\overline{\gamma}$ (see Fig. 4-bottom).

2.2 Observing the phase transition

Experiment A Starting from a random initial configuration, we set the control parameters $\alpha \in [0, 2]$ and $\rho = 0.2$, and let the system evolve for a few hundred steps. We observe two qualitatively different behaviours:

- For "intermediate" values of the swarming sensitivity $\alpha \in [1, 2]$, the system evolves according to the diagonal stripe pattern described before. Due to the nature of the observed configurations, this phase is referred to as *ordered*[2].

[2]In the literature, disordered and ordered phases have been refered as *stable* and *unstable*,

- When α is below a critical value $\alpha_c \sim 1$, the system does not seem to show any emergent behaviour. Both mean velocity and mean alignment remain near-zero, and the configuration remains visually indistinguishable from a random distribution (see top row of Fig. 4). This phase is referred to as *disordered*.

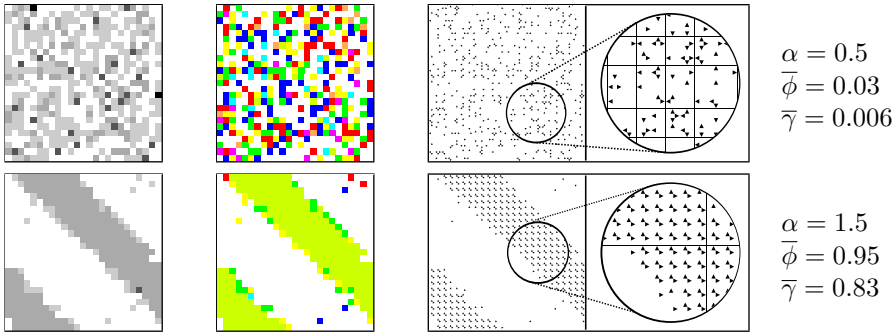

Figure 4: Observation of a random distribution (top) and the diagonal stripe (bottom) pattern. The visualisation are particle density (left), flux (middle) and channels (right), for $L = 25,\ t = 1000,\ \rho = 0.2$.

A quantification of this discontinuous shift of behaviour for $\rho = 0.2$ is displayed on Fig. 5-left. The sharp change in the value of the mean alignment $\overline{\gamma}$ for a critical value of the alignment sensitivity α_c corresponds to the transition from no apparent pattern to the system self-organisation.

2.3 Construction of the phase diagram

Using the same criteria as in Experiment A, it was observed that for different values of the initial density ρ, the critical sensitivity α_c was different. This phenomenon, known as the *swarm instability* appears on Fig. 6 as a parametric line separating the disordered phase, in which the particles remain randomly distributed on the lattice, and the ordered phase, where particles start gathering into clusters.

Bussemaker *et al.* studied the initialisation of swarming through a mean-field analysis [11]: under the assumption of a spatially homogeneous, isotropic and stationary solution with respect to local fluctuations, they established the values of the particle density and alignment sensitivity for which the transition occurs. These values are represented by the dashed line on Fig. 6. Our observations of the swarm instability are in general agreement with this parametric line, though they show that a difference exists for the trigger values of the swarm instability for low values of the initial density ρ.

respectively. We renamed them so, as stability may either refer to the evolution from a pattern to another, or to the stability of the pattern themselves.

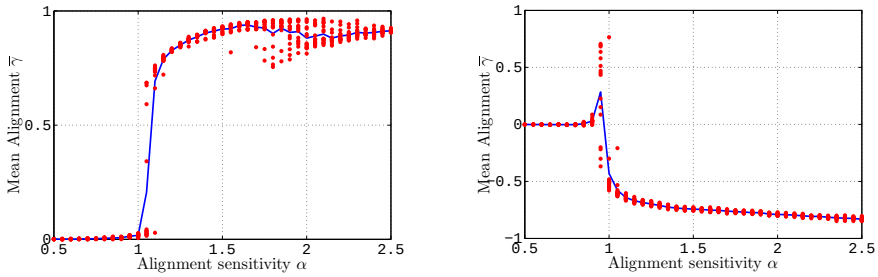

Figure 5: Visualisation of the phase transition using the mean alignment parameter for $\rho = 0.2$ (left) and $\rho = 0.4$ (right). The values are obtained from 32 simulations for each value of α, with size $L = 50$ and for 5000 steps. The dots corresponds to single simulations, and the line to their average.

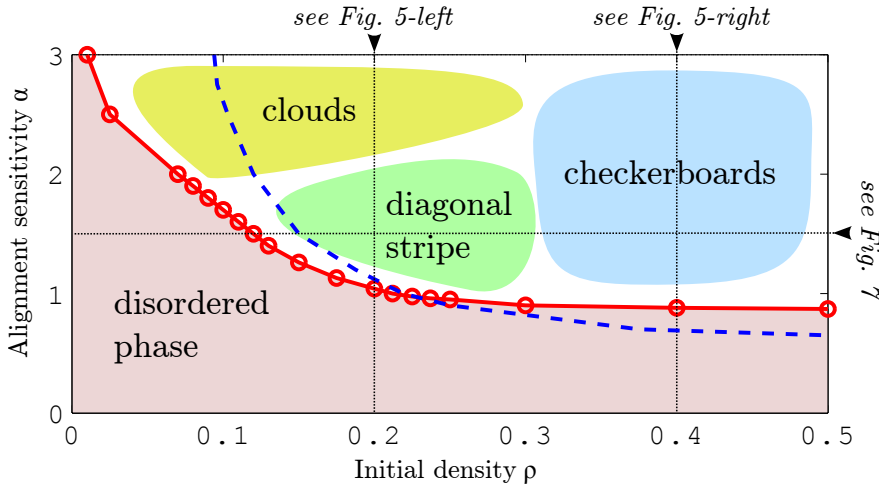

Figure 6: Spatial distribution of the disordered and ordered phases in the density-sensitivity parametric plane. We divided the ordered phase into approximated regions of appearance of observed patterns (see Sec. 3). Circles designates our own measurements of the swarm instability phase transition. The dashed curve is derived from Bussemaker *et al.* [11].

This diagonal stripe pattern is an emergent behaviour that embodies the kind of global behaviour expected from a swarming model. When this pattern is formed, particles manage to aggregate and move collectively in consensual directions. This argument is supported by the high values and stability of the order parameters, which suggest that: (a) almost all particles are aligned and (b) a consensus on the directions is found globally. For this reason, we will consider thereafter that the diagonal stripe pattern is the "reference behaviour" of swarming.

3 Novel phenomena in the swarm instability

In this section, we show that stressing the model by using extreme values for the parameters makes unexpected patterns emerge. Here the question of the robustness of the diagonal stripe pattern is central, as we will show that it is not the only possible behaviour for the ordered phase.

3.1 Particle saturation of the lattice

Experiment B Keeping the alignment sensitivity α fixed, we gradually increase the initial density of particles ρ and observe the evolution of the order parameters. Figure 7 plots a repartition of long-run configurations according to their initial density and the resulting mean alignment. First observation: for low values of the initial density $\rho \in [0; 0.3]$, the value of the mean alignment $\overline{\gamma}$ is in agreement with the observations of the swarm instability made in Sec. 2. The segment a on Fig. 7 corresponds to a random distribution of particles, whereas the segment b is determined as the diagonal stripe pattern.

However, simulations for higher values of ρ show an unexpected change in the values of the mean alignment $\overline{\gamma}$, meaning that the system has adopted a behaviour that does not correspond to the diagonal stripe pattern. We observe the occurrence of a sharp transition[3] in the continuous domain of the initial density ρ. This observation is confirmed, by fixing $\rho = 0.4$ and simulating for different values of α, where one can notice a transition for which the value of the mean alignment $\overline{\gamma}$ diverges for a critical value of α, and then converges to a negative value (see Fig. 5-right). By observing the simulation for this parameters setting, we found out that two novel patterns emerge:

Checkerboard pattern. For $\rho \in [0.3, 0.5]$ (segment c on Fig. 7), the system tends to organise into regions where each cell contains two particles that are antialigned (see Fig. 8-top). We call this pattern "checkerboard" as the observation with the flux visualisation displays patterns of alternating "opposite colors", revealing that neighbouring cells are antialigned. This observation is confirmed by a negative mean alignment $\overline{\gamma}$.

[3] The reproduction of this brutal change of behaviour independently of the size of the lattice pleads for a phase transition phenomenon.

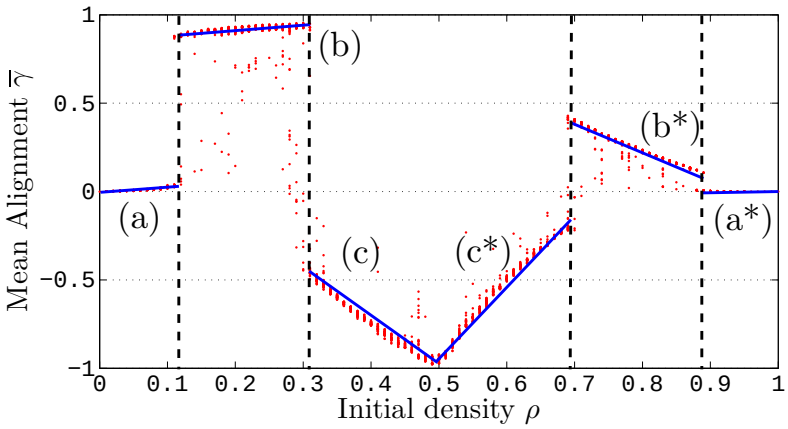

Figure 7: Visualisation of multiple phase transitions using the mean alignment parameter for $\alpha = 1.5$. The values are obtained from 64 simulations for each value of ρ, with size $L = 100$ and for 10 000 steps. Vertical lines show phase transitions and dots corresponds to values obtained in single simulations.

Hybrid pattern. This pattern occurs in some configurations, for values of the initial density even closer to $\rho = 0.5$. It can be interpreted as an hybridisation of "one-dimensional patterns", that is, patterns of particles along one dimension: for one direction, particles are aligned with their neighbours, but for the orthogonal direction they are antialigned (see Fig. 8-middle). Consequently, this pattern can quantified by a near-zero mean alignment $\overline{\gamma} \sim 0$ and a mean velocity $\overline{\phi} \sim 0.5$.

Interpretation For particle densities in the vicinity of $\rho = 0.5$, a diagonal stripe – as it is composed of 2-particle cells of same flux – would cover the entire lattice, leaving almost no empty cells. But as observed previously, the formation of a diagonal stripe pattern requires interactions between traveling clusters of collinear particles over several periods. With so little empty space, these clusters are steadily influenced by conflicting fluxes and never reach a consensus. In some sense, it is just as if the system was so saturated with particle interactions that it could not form a diagonal stripe pattern, and "prefers" to stabilise in a checkerboard pattern. The stability of the checkerboard patterns can be understood by considering a configuration sample made of cells set in a checkerboard pattern as shown on Fig. 9.

A symmetry by complementation Another peculiar observation is made for higher values of the initial density: as seen on Fig. 7, the behaviour appears to be symmetrical around the axis $\rho = 0.5$. This observation is confirmed by visual observation of the patterns on each side of the ρ-axis (segments a and

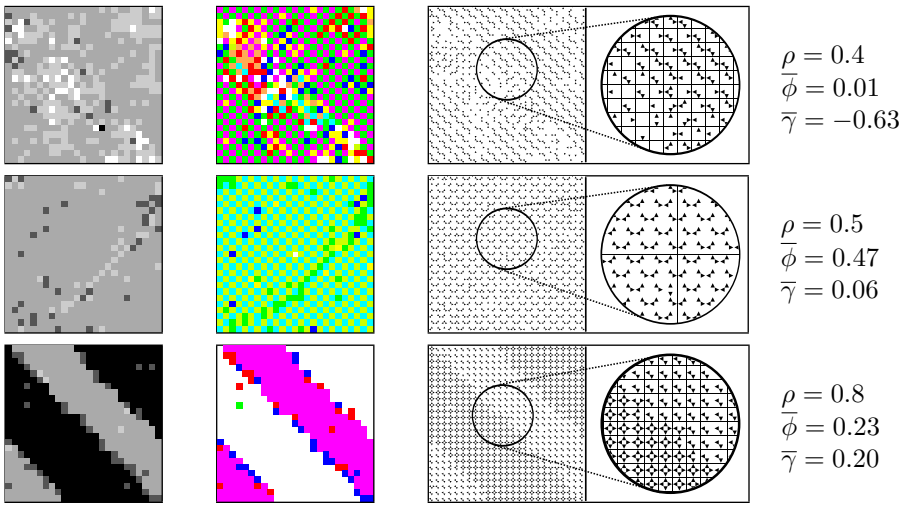

Figure 8: Observation of the checkerboard (top), hybrid (middle) and the negative diagonal stripe (bottom) patterns, for $L = 25,\ t = 1000,\ \alpha = 1.5$.

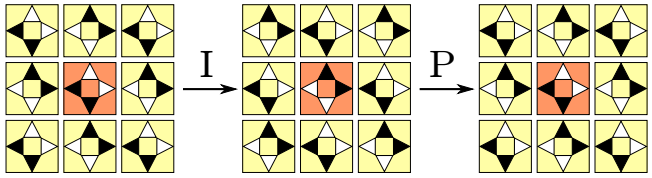

Figure 9: Step-by-step analysis of a sample of checkerboard pattern. Note that the resulting state is identical to the initial one after the interaction and propagation steps are applied.

a^*, b and b^*, c and c^*). An example of such "reversed" pattern is given on Fig. 8-bottom where a reversed diagonal stripe pattern can be observed, that is, the system evolves into a stable pattern formed of *empty channels*.

This phenomenon can actually be explained by noting that, if we consider $\boldsymbol{x}^*$ the inverse configuration of $\boldsymbol{x}$ such that $x_i^*(c) = 1 - x_i(c)$, for all $i \in \{1, ..., \nu\}$ the probability for the interaction transition to update from a configuration $\boldsymbol{x}$ to $\boldsymbol{x}^I$ is the same than from $\boldsymbol{x}^*$ to $\boldsymbol{x}^{*I}$. Formally, as $\boldsymbol{J}_c(\boldsymbol{x}^*) = -\boldsymbol{J}_c(\boldsymbol{x})$, we thus have $\boldsymbol{D}_c(\boldsymbol{x}^*) = -\boldsymbol{D}_c(\boldsymbol{x})$, which gives $P(\boldsymbol{x}_c^* \to \boldsymbol{x}_c^{*I}) = P(\boldsymbol{x}_c \to \boldsymbol{x}_c^I)$ (see Eq. 3, 4, 6). As a consequence, a configuration with $\rho > 0.5$ will have the same evolution as its inverse by complementation, which explains the apparition of the symmetrical patterns. The difference in the values of the mean alignment $\overline{\gamma}$ on both sides of the symmetry axis comes from the use of an average over the total number of particles during its measure.

3.2 High alignment sensitivity

Experiment C Let us now fix the initial density to a value $\rho = 0.2$ as in Experiment A, and this time focus on increasing further the value of the alignment sensitivity α (*e.g.* $\alpha > 4$). Intuitively, this means that we widen the gaps between interaction probabilities (see Eq. 6). There again, we observe that for a high value of α, two distinct novel patterns appear for the same parameter settings:

Clouds pattern. In such configurations, the system quickly evolves into a small number of clusters of collinear particles (see Fig. 10-top). These clusters travel through the lattice and meet by overlapping occasionally, but the probability for a particle to leave its cluster for another is so low that the pattern is actually stable in the long run. It is characterised by a high mean alignment $\overline{\gamma}$ while the mean velocity $\overline{\phi}$ can take any value in $[0, 1]$, as non-conflicting clusters of opposing directions can co-exist.

Cross pattern. This pattern is made of two distinct clusters of cells, one horizontal and the other vertical, where each cell contains at least one particle that is antialigned with its neighbours (see Fig. 10-bottom). Contrarily to the clouds pattern, this pattern is static, and is characterised by a near-zero mean velocity $\overline{\phi}$ and a negative mean alignment $\overline{\gamma}$.

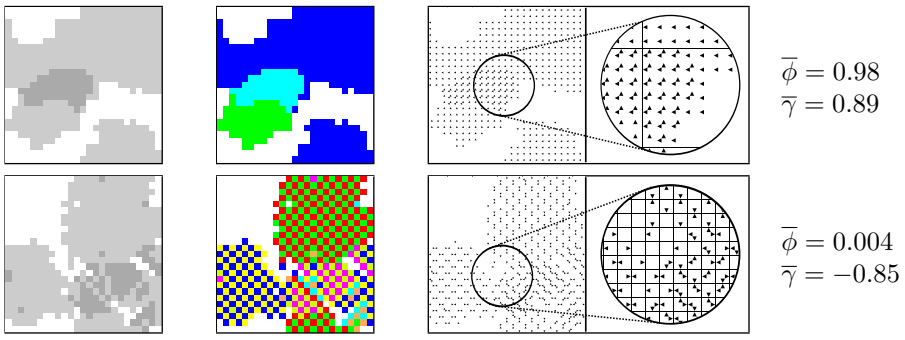

Figure 10: Observation of the clouds (top) and cross (bottom) patterns, for $L = 25,\ t = 1000,\ \rho = 0.2,\ \alpha = 4$.

Interpretation How can we explain the apparition of novel patterns for a high alignment sensitivity? When α increases, the gaps between probabilities of each cell states of the interaction step are amplified, making the system less likely to select configurations that would not maximise the local alignment. As displayed in Fig. 2, for $\alpha = 4$, the cell configuration that has the highest probability to be selected is associated with a probability 1000 times higher than the second most likely. As a result, the system becomes more "deterministic",

and where clusters of collinear particles were interacting until a diagonal stripe pattern was formed, we now observe two different patterns.

This observation suggests that a too high alignment sensitivity has the *reverse* effect of favoring the swarming behaviour: it actually settles the system to a "sub-optimal" state where clusters of particles can no longer influence each other to maximise their alignment.

4 Dependence of patterns on the lattice properties

We now estimate the robustness of the patterns by using different lattices in order to gain insight on how the spatial regularity of the topology influences the stability of behaviours.

Experiment D: Dependence on the lattice size We repeated all previous simulations doubling the lattice size. Surprisingly, the hybrid and cross patterns were no longer observed, which suggests that they become less frequent as the lattice size increases. As a result, patterns can be classified into two groups:

- Size-independent patterns, which will appear more often, and almost always for large lattices. This comprises the diagonal stripe (for small densities), the checkerboard and the clouds patterns.
- Size-dependent patterns, which are more likely to occur in small-size lattices and are most likely related to finite-size effects. This includes the hybrid and cross patterns, and the diagonal stripe (for high densities).

Experiment E: Dependence on the lattice shape One may then wonder what happens when the lattice has unequal values for its dimensions. We took a rectangular lattice $\mathcal{L} = (\mathbb{Z}/L_x\mathbb{Z}) \times (\mathbb{Z}/L_y\mathbb{Z})$, where L_x and L_y are respectively the width and height of the lattice. Trying different ratios for L_x and L_y revealed no significant modification for any pattern, save the diagonal stripe. The system then organises into an unfinished, distorted diagonal stripe pattern that yet manages a certain degree of stability (see Fig. 11-left). This modification can be easily understood since the shape of this pattern cannot loop "regularly" over the periodic boundaries, and cannot exist as described earlier.

In order to quantify this phenomenon, we took the same experimental conditions as in Experiment A: we fixed $\rho = 0.2$ and, for different values of the alignment sensitivity α, measured the mean alignment $\overline{\gamma}$ of the configuration after a few hundreds steps. Every ratio we used reproduced the phase transition between the disordered and the ordered phases, though the plot profile and the critical value α_c slightly differed (see Fig. 11-right). We observed that, for different "types" of ratios, different plot profiles appeared:

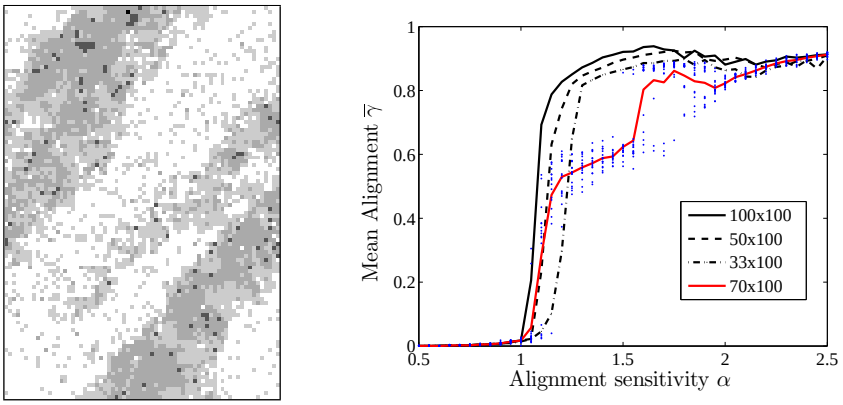

Figure 11: Left: a sample configuration for a lattice of geometry 70×100 at time $t = 5000$. Note the irregularity of the diagonal stripe. Right: the swarm instability phase transition for different lattice geometry ($L_y = 100$). Dots designates single simulations.

- Harmonic or quasi-harmonic ratios (*e.g.* 100×100, 50×100, 33×100) show a "regular" phase transition in which the diagonal stripe pattern can loop over periodic boundaries several times in a most regular way.
- For other ratios (*e.g.* 70×100), the plot profile suggests that a second transition occurs for a higher value of the alignment sensitivity, which we identified as the transition from diagonal stripe to cloud patterns.

Interpretation These observations support the hypothesis of a strong connection between the formation of the diagonal stripe pattern and the regularity of the lattice. The diagonal stripe pattern is formed from the periodic interactions of clusters, which compete and grow until they find a consensual configuration. To some extent, this can be considered as a "resonance" effect caused by the limited size of the system, coupled with the periodic boundaries condition.

The shape of the lattice is just one aspect of the lattice definition. Yet they manage to display how some of the observed patterns depend on properties of the model. Variations on different boundary conditions as well as the topology are also important, and their study is left for future work.

5 Discussion and perspectives

With regard to the previous studies on this model, how can we interpret our observations of the novel behaviours in the context of models of biological systems? We now discuss this question by considering the following points:

Connections between patterns We have presented the patterns as differentiated behaviours based on visible changes in the order parameters. However, from a different perspective, one may observe that they are the result of the superposition of two "one-dimensional patterns", by projection of the particles orientation on each of the two axes of the lattice. Along one dimension, the system may either organise in groups of aligned particles (*e.g.* clouds, diagonal stripe pattern) or may "prefer" antialigned particles (*e.g.* checkerboard, cross patterns). The hybrid pattern is an example of a cohabitation between two one-dimensional patterns. Studying the behaviour along one dimension while neglecting interactions in the other may give us insight on the formation of patterns.

Metastability of patterns Our simulations showed that various patterns could appear depending on the initial density ρ or the alignment sensitivity α (see summary in Tab. 1), but as they were limited in time, they did not capture how stable the presented patterns are or how often they occur. We know that in some cases, patterns can exist but their occurrence in a short "reasonable" simulation time is highly unlikely (*e.g.* the diagonal stripe for high densities, the cross for large lattices). Our belief is that the presented patterns are subject to phenomena of *metastability* [14, 19]: from an initial unstable configuration, the system evolves towards one of the possible equilibria and once one has been reached, the system will hold it until random fluctuations allow it to "escape" the stable state in very long times. Quantifying the stability of patterns with regard to the settings in the control parameter domain is an interesting open problem.

Characterising the phase transitions Another open issue stands about the nature of the swarm instability: if Csahók *et al.* [13] have claimed that the phase transition was "weakly first-order", Bussemaker *et al.* [11] reckon that it is second-order. Our approach, based on simulations of finite-size periodic lattices, reveals various stable behaviours and the existence of multiple phase transitions (see Fig. 7). We consider observed patterns as meta-stable states, which pleads for first-order transitions between behaviours. The problem we are now facing is to interpret the current results, obtained for finite size, in the case of infinite systems. This problem becomes obvious in the case of the diagonal stripe pattern, which clearly appears as a resonance effect that can only exist in finite systems. Similarly, the novel transitions between patterns we observed raise the question of whether they are phase transitions and how to characterise them. The interpolation of the system's behaviour to infinite lattices could be obtained by setting a time of simulation adequate to the lattice size, and is left for future work.

Revealing and overcoming discretisation effects By simulating the model in a parameter range that was not planned by its original purpose, we uncovered unexpected behaviours. For instance, antialigned patterns are all the more sur-

pattern name	Random	Diagonal stripe	Checker-board	Hybrid	Clouds	Cross
α	0.5	1.5	1.5	1.5	4	4
ρ	0.2	0.2	0.4	0.5	0.2	0.2
density visual.	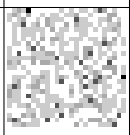	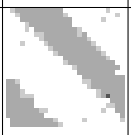	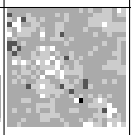	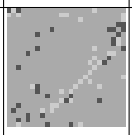		
orientation visual.	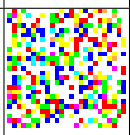	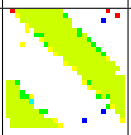	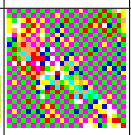	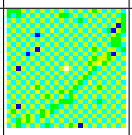	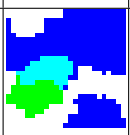	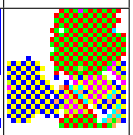
$\overline{\phi}$	0.03	0.95	0.01	0.47	0.98	0.004
$\overline{\gamma}$	0.006	0.85	-0.63	0.06	0.89	-0.85
pattern is mobile	random	yes	no	one axis	yes	no
pattern frequency	always	often	often	rare	often	rare

Table 1: Summary of the observed patterns.

prising as they are in *opposition* of what would be expected from an alignment-maximising rule: although particles try to maximise their own alignment, the global alignment remains negative. To explain this phenomenon, a plausible hypothesis lies in that by "pushing" these parameters, we reduce the "degrees of freedom" of cells and exacerbate certain aspects of the individual behaviour at the expense of other possibilities. For instance, a high sensitivity (*e.g.* $\alpha \sim 4$) amplifies the alignment maximisation, and a high density (*e.g.* $\rho \sim 0.5$) reduces the number of alignment possibilities by saturating the lattice. Thus, stressing the model has the effect of enhancing the discretisation effects that were originally "softened" by the stochasticity of the model.

A possible solution to overcome discretisation and model-related biases in the model consists of making the system more stochastic. For example, by extending the concept of asynchronism for cellular automata to the LGCA interaction rule, that is, by applying the interaction rule with a given probability, and leaving it unchanged otherwise. This type of perturbations could add the necessary noise for the system to "break" patterns such as checkerboards.

Conclusion

We have shown that for this LGCA model, the ordered phase of the swarm instability could not be reduced to the sole emergence of a diagonal stripe pattern. Considering a broader range of the parameter domain, and introducing new ways to monitor the evolution of the system, we uncovered patterns that

account for qualitatively different behaviours of the system.

This confirms that this model of swarming is a complex system: although the local rule is simple, the global behaviour is difficult to predict from the interactions of components. The simplification of the original phenomenon was intended to rid the model of the system from properties that are not relevant for the phenomenon we study. This allows a faster exploration of the model and a better understanding of the mechanisms responsible for the emergent behaviour. However, as our observations suggest, the system is also subject to influences from certain properties of the simplified model, which "alter" the emergent behaviour. The challenge for the observer lies in the distinction between which behaviour is an artifact caused by a discretisation of the model, and which is related to the phenomenon studied. In short, in the context of simulations of biological systems with discrete dynamical systems, it is of prime importance to explore the robustness of the behaviour, in order to identify the potential artifacts induced by the discretisation of the model.

References

[1] C. W. Reynolds, Flocks, herds, and schools: A distributed behavioral model, Computer Graphics 21 (4) (1987) 25–34.

[2] J. Kennedy, R. C. Eberhart, A discrete binary version of the particle swarm algorithm, Systems, Man, and Cybernetics 5 (1997) 4104–4108.

[3] H. Leung, R. Kothari, A. A. Minai, Phase transition in a swarm algorithm for self-organized construction, Physical Review E 68 (4) (2003) 046111.

[4] S. Whitelam, E. H. Feng, M. F. Hagan, P. L. Geissler, The role of collective motion in examples of coarsening and self-assembly, Soft Matter 5 (2009) 1251–1262.

[5] B. Chopard, R. Ouared, A. Deutsch, H. Hatzikirou, D. Wolf-Gladrow, Lattice-gas cellular automaton models for biology: From fluids to cells, Acta Biotheoretica 58 (2010) 329–340.

[6] H. Hatzikirou, L. Brusch, C. Schaller, M. Simon, A. Deutsch, Prediction of traveling front behavior in a lattice-gas cellular automaton model for tumor invasion, Computers Mathematics with Applications 59 (7) (2010) 2326–2339.

[7] D. Helbing, M. Isobe, T. Nagatani, K. Takimoto, Lattice gas simulation of experimentally studied evacuation dynamics, Physical Review E 67 (2003) 067101.

[8] A. Lerner, Y. Chrysanthou, D. Lischinski, Crowds by example, Computer Graphics Forum 26 (3) (2007) 655–664.

[9] T. Vicsek, A. Czirók, E. Ben-Jacob, I. Cohen, O. Sochet, Novel type of phase transition in a system of self-driven particles, Physical Review Letters 75 (1995) 1226.

[10] F. Peruani, A. Deutsch, M. Bär, A mean-field theory for self-propelled particles interacting by velocity alignment mechanisms, The European Physical Journal - Special Topics 157 (2008) 111–122.

[11] H. J. Bussemaker, A. Deutsch, E. Geigant, Mean-field analysis of a dynamical phase transition in a cellular automaton model for collective motion, Physical Review Letters 78 (26) (1997) 5018–5021.

[12] A. Deutsch, S. Dormann, Cellular Automaton Modeling of Biological Pattern Formation, Birkhauser Boston, 2005.

[13] Z. Csahók, T. Vicsek, Lattice-gas model for collective biological motion, Physical Review E 52 (1998) 5297–5303.

[14] H. Kitano, Biological robustness, Nature Reviews Genetics 5 (2004) 826–837.

[15] R. M. D'Souza, Coexisting phases and lattice dependence of a cellular automaton model for traffic flow, Physical Review E 71 (2005) 066112.

[16] A. Kirchner, H. Klüpfel, K. Nishinari, A. Schadschneider, M. Schreckenberg, Discretization effects and the influence of walking speed in cellular automata models for pedestrian dynamics, Journal of Statistical Mechanics: Theory and Experiment 2004 (10) (2004) P10011.

[17] B. H. Schönfisch, M. O. Vlad, Finite-size scaling for cellular automata with randomized grids and for fractal random fields in disordered systems, Internat. J. Modern Phys. B 10 (5) (1996) 523–542.

[18] C. Grilo, L. Correia, Effects of asynchronism on evolutionary games, Journal of Theoretical Biology 269 (1) (2011) 109–122.

[19] E. Cirillo, F. Nardi, C. Spitoni, Metastability for reversible probabilistic cellular automata with self-interaction, Journal of Statistical Physics 132 (2008) 431–471.